J Mater Sci (2007) 42:465–471
DOI 10.1007/s10853-006-1170-9

Synthesis and characterization of ordered and cubic mesoporous silica crystals under a moderately acidic condition

Zhengwei Jin · Xiaodong Wang · Xiuguo Cui

Received: 22 August 2005 / Accepted: 22 February 2006 / Published online: 28 November 2006

Abstract Ordered and cubic mesoporous silica materials were synthesized by using poly(ethylene oxide-*b*-propylene oxide-*b*-ethylene oxide) triblock copolymer as template under a moderately acidic condition of 0.5 mol/l HCl solution. These mesoporous materials were characterized by Fourier transform (FT) IR spectroscopy, thermo-gravimetric analysis (TGA), X-ray diffraction (XRD) pattern, scanning electron microscopy (SEM), transmission electron microscopy (TEM), and nitrogen adsorption–desorption measurements. The three-dimensional cage-like microporosity of the prepared mesoporous silica having ordered hexagonal mesoporous structure was evidenced by the well-defined XRD patterns combined with TEM photographs. SEM observation shows a highly regular cubic crystal structure for the prepared mesoporous silica. The size of these crystallites was maintained within the range between 4 and 6 μm, which is fairly important for the application to the stationary phase for separation. The nitrogen adsorption–desorption analysis reveals that the prepared mesoporous silica possesses a small pore diameter of 3.68 nm, a total surface area of 363.648 m^2/g, a total pore volume of 0.379 cm^3/g, and a pore-wall thickness of 6.63 nm. These features may lead to higher thermal and hydrothermal stability, excellent microporosity, and good connectivity. The mesoporous silica prepared in this study exhibits potential applications to catalysis, sensoring, and separation.

Z. Jin · X. Wang (✉)
Key Laboratory of Beijing City on Preparation and Processing of Novel Polymer Materials, School of Materials Science and Engineering, Beijing University of Chemical Technology, Beijing 100029, China
e-mail: wangxdfox@yahoo.com.cn

X. Cui
Department of Chemical Engineering and Polymer Science, Yanbian University, Yanji City, Jilin 133002, China

Introduction

Since the scientists of Mobil Company discovered that a family of mesoporous siliceous materials, which were called M41S, could be synthesized by using cationic surfactants as templates [1, 2], there has been an increasing interest in the design of novel porous materials tailored with various ordered pore organization and dimensions for potential applications in separation, catalysis, chemical sensing, and low dielectric and optical coatings [3, 4]. In view of the extensive applications of these materials, the production of novel structures and novel synthesis procedures for them is of great interest. One of the most studied mesoporous materials is MCM-41, which has unidirectional mesopores ordered in an hexagonal array and a sharp pore size distribution, and can be obtained using ionic surfactants in dilute (micellar) or liquid crystalline solutions [1]. These ordered hexagonal mesoporous materials have attracted considerable interest in applications of molecular sieves, catalysts, adsorbents and sensors due to their orientation and uniformity [5, 6]. In addition, they provide excellent opportunities for the creation of materials with additional functionality. Their regular pore system can be used to introduce molecules or particles that are stabilized by the solid framework and are spatially organized by the regular

pore system. The inorganic frameworks of the host systems have several interesting material properties, which make them highly suitable for the construction of advanced materials, including their optical transparency in the visible and near ultraviolet range and their high thermal stability [7].

Recently, mesoporous materials, with larger pore size and better stability as compared to the M41S materials, were synthesized by employing the template of commercially available nonionic poly(ethylene oxide-*b*-propylene oxide-*b*-ethylene oxide) (EO_n–PO_m–EO_n) triblock copolymer reported by D. Y. Zhao et al. in 1998 [8, 9]. These novel mesoporous materials denote SBA-n silicas, and exhibit two and three dimensional hexagonal (SBA-2, 12, 3, 15) [10–12] and cubic (SBA-1, 6, 16) pore architectures [13–15]. The cubic phase mesoporous silica SBA-16 ($Im\ \bar{3}m$) possesses a three-dimensional channel system and uniform-sized pores of exceptionally large cage-like structure with cubic symmetry. It is well known that mesoporous silica materials are synthesized by synergistic self-assembly between surfactant and silica species to form mesoscopically ordered structures. These substrates are prepared through the micelle-templating technique by seeding spherical surfactant aggregates during the synthesis of a SiO_2 sol performed by the hydrolysis of tetraethoxysilane (TEOS) [16, 17]. The micelles are later entangled within the ensuing gel environment and could leave holes inside the amorphous silica phase after being eliminated by a subsequent thermal treatment. Numerous literatures reported that the mesopore cage-type mesoporous silica, designated as SBA-16 [13, 18, 19] or FDU-1 [20], could be synthesized in a strongly acidic media (usually 2.0 mol/l HCl solution) with EO_n–PO_m–EO_n triblock copolymer as the template, and with TEOS as the silica source. Apparently, such a strongly acidic condition is directly related to an assembled condition of the templating surfactant through micelle controlling, which determines the mesopore cage-type structure. Typical cage-like substrates consist of spherical cavities of 6–10 nm in diameter arranged in the form of a body-centered cubic array (i.e. with $Im\ \bar{3}m$ symmetry), and are connected through mesoporous openings of 2.0–2.5 nm which lie along the crystallographic (111) plane. Due to the symmetry of the arrangement, each spherical cavity is surrounded by eight neighboring voids; pairs of nearest neighbor voids are linked through narrow necks alongside the (111) direction [21, 22]. Because of the exceptionally large cage, high surface area, high thermal stability and, especially, the three dimensional channel connectivity which provides more favorable mass transfer kinetics than the unidirectional pore system of other hexagonal mesoporous phases, SBA-16 is considered to be suitable for catalyst supports, thin films, and packing materials for separation [23, 24]. However, such a strongly acidic synthesis condition mentioned preciously does not favor industrial production of the mesoporous silica materials like SBA-16.

In this study, we report the synthesis of a cage-like SBA-16-type cubic mesoporous silica by using nonionic surfactant EO_n–PO_m–EO_n triblock copolymer as the template under a moderate acidity (0.5 mol/l HCl solution). The prepared mesoporous silica has a highly perfect body-center cubic crystal architecture with highly ordered mesopores, and the structure of the product was systematically investigated.

Experimental

Chemicals

Poly(ethylene oxide-*b*-propylene oxide-*b*-ethylene oxide) triblock copolymer (EO_{132}–PO_{50}–EO_{132}, F108) was commercially obtained from the BASF Company. TEOS was supplied by Beijing Chemical Reagents Company. HCl, and potassium sulfate (K_2SO_4) were purchased from the Tianjin No. 3 Chemical Reagent Company. Ethanol (99.7 wt.-%) was purchased from the Atoz Fine Chemicals Co., LTD. All of the chemicals were used without any further purification.

Synthesis of specimens

In a typical synthesis, 1.25 g of F108 and 2.10 g of K_2SO_4 were dissolved in 30 g of 0.5 mol/l HCl solution at 35°C. The pH value of the solution kept in around 0.3. About 4.2 g of TEOS was dropped slowly into the template solution under moderate stirring for 24 h at the same temperature while continuously stirring, until a transparent solution formed. After that, the solution was stored at 35°C for 24 h to obtain deposition, and then at 80°C for 24 h for the post-treatment. The precipitate obtained from the solution was washed by de-ionized water and alcohol, and dried in air for more than 7 days at room temperature. The resulting powders were calcined at 550°C for 6 h to remove the template.

Characterization

X-ray diffraction patterns (XRD) were obtained using a Japan Rigaku D/max-r C instrument with Cu Kα radiation (40 kV, 50 mA). Scanning electron microscopy (SEM) was performed on a Japan Hitachi

S-3500N instrument. Transmission electron microscopy (TEM) was acquired from a Japan Hitachi S-4200 instrument operating at 120 kV. The nitrogen adsorption and desorption isotherms were measured on a Micrometeritics ASAP2020 volumetric adsorption analyzer. Before the adsorption measurements, the sample was outgassed under vacuum for 11 h at 300°C. The pore volumes and diameter distributions were measured by the Brunauer–Joyner–Halenda (BJH) method. The surface area was calculated by Barrett–Emmett–Telleller (BET) mode. Thermogravimetric analysis (TGA) was performed on a Perkin Elmer TGA 7 apparatus from 35°C to 700°C in a nitrogen gas atmosphere with heating rate of 10°C/min. Infrared (IR) spectra were obtained using a Perkin-Elmer 1730 Fourier transform (FT) IR spectroscopy apparatus. The sample was mixed with KBr and pressed as pellets at 25°C.

Results and discussion

Figure 1 presents the FTIR spectra of as-synthesized and calcined samples prepared in this study. Bands at 1090 and 795 cm^{-1} belonging to the asymmetric and symmetric stretching vibrations, respectively, corresponding to the Si–O–Si framework could be observed from the IR spectrum of the as-synthesized samples. The intense band at 3466 cm^{-1}, as well as the weak band at 968 cm^{-1} represent Si–OH stretching and bending vibrations, respectively. Since the sample we prepared has been synthesized through synergistic self-assembly between surfactant (EO_{132}–PO_{50}–EO_{132} triblock copolymer) and silica resource (TEOS) to form mesoscopically ordered composites, it was formed via a condensation of silanols along the micellar surface of the surfactant in an acidic media. It is expected that a large quantity of silanol groups should be detected on their inorganic walls. It is evident that the IR spectrum of the as-synthesized samples confirms these silanol groups (Si–OH). For the calcined sample, the band at 1090 cm^{-1} becomes broad, but its position remains unchanged, and the band at 795 cm^{-1} shifts to a higher wave number (807 cm^{-1}) because of structural contraction, which has been confirmed by the XRD patterns of the samples as discussed in following section. It is deduced that the condensation between the silanol groups proceeds further during the calcination. This reduces the concentration of silanols and consequently results in a shift of the band at 795 cm^{-1} to a higher wave number. Furthermore, the intensity of the absorption peak of silanol groups at 3466 cm^{-1} weakens in comparison with that of the as-synthesized sample, which is attributed to further condensation of silanols during calcination. It is also observed that absorbance peaks corresponding to C–H stretching (2850–3000 cm^{-1}) and bending (1375 and 1290 cm^{-1}) vibrations of the triblock copolymer within the pores of the prepared mesoporous silica have disappeared after calcination, which implies the complete removal of the surfactant.

The TGA measurements of the surfactant and the as-synthesized sample were carried out in a nitrogen gas atmosphere, and the thermal degradation behaviors are displayed in Fig. 2. The surfactant shows a typical one-step degradation for thermoplastic polymers with a rapid weight loss at a temperature of about 250°C and a char ratio of 0%. However, the as-synthesized sample

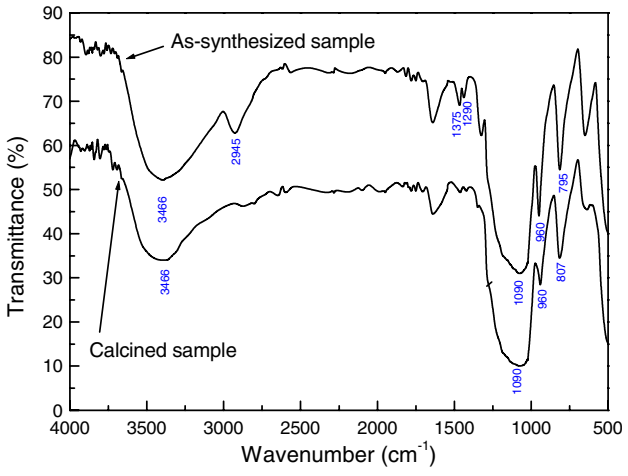

Fig. 1 Fourier transform IR spectra of the as-synthesized and the calcined mesoporous silicas prepared in a moderately acidic medium

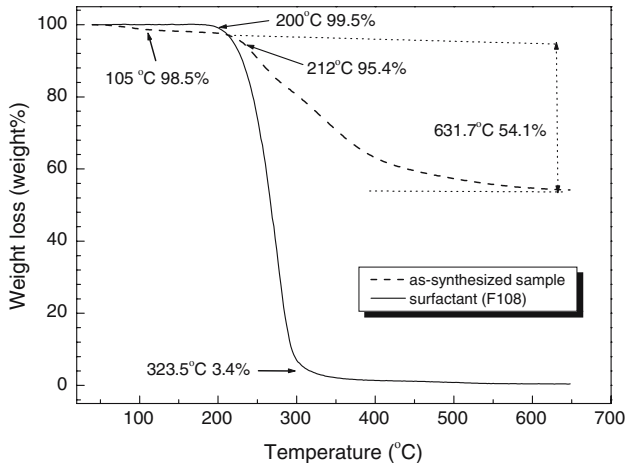

Fig. 2 Thermogravimetic analysis (TGA) thermograms of the surfactant (F108) and the as-synthesized sample in a nitrogen gas

exhibits three weight loss steps in the TGA curve with a total weight loss of 58.7 wt.%. The weight loss near 105°C (1.5 wt.% loss) is assigned to water desorption, whereas the weight losses at 212°C (4.1 wt.% loss) and 450°C (32.4 wt.% loss) are assigned to desorption and decomposition of the surfactant, respectively. By 632°C, essentially all of the nonionic organic surfactant has been removed from the channels of the prepared sample, and the remanent inorganic material exhibits a good thermal stability.

Figure 3 displays the XRD patterns of the as-synthesized and the calcined samples prepared in this study. It is found that the as-synthesized specimen exhibits a well-resolved diffraction peak and a series of broad diffraction peaks with low intensity, in which the single well-resolved diffraction peak at $2\theta = 0.95°$ could be clearly assigned to (110) plane of the crystal of the prepared samples. From the magnified curve of the as-synthesized sample, three minor diffraction peaks were observed at $2\theta = 1.26°$, 1.54° and 1.92°, which correspond to the (200), (211), and (220) planes of the crystal. From Bragg's law ($n\lambda = 2d \sin\theta$) and the relationship $[1/d^2_{(hkl)} = (h^2 + k^2 + l^2)/a^2]$ between the cubic lattice parameter (a) and interplanar distance ($d_{(hkl)}$) for given different Miller indices (hkl), some interplanar distances for the as-synthesized sampled were calculated as to be $d_{(110)} = 9.20$ nm and $d_{[200]} = 6.64$ nm, and the cubic lattice parameter was calculated to be $a = 9.2 \times \sqrt{2} = 13.0$ nm. These experimental and calculated data indicate a cubic ($Im\ \bar{3}m$) structure for the prepared sample, and agree with the results reported in the literature [18, 19]. For the XRD patterns of the calcined sample, a single well-resolved diffraction peak corresponding to (110) plane was also found at a 2θ value of 1.04°. Moreover, a series of minor diffraction peaks were found to be indexed as (200), (211), (220), (310), and (222) planes (see upper curves in Fig. 3), in which the corresponding diffraction peaks shifted to higher 2θ value. These results reveal that the calcined sample has a highly ordered mesostructure. However, the interplanar distances and the cubic lattice parameter for the calcined sample were calculated to be $d_{(110)} = 8.47$ nm and $d_{(200)} = 6.20$ nm, and $a = 8.47 \times \sqrt{2} = 11.9$ nm. It is evident that the reduction of the structure spacings resulted from the elimination of the template (triblock copolymer), and the condensation of silicon hydroxyl groups during the calcination of the prepared sample. The reduction ratio of $d_{(200)}$ as a result of calcination was 8.46%.

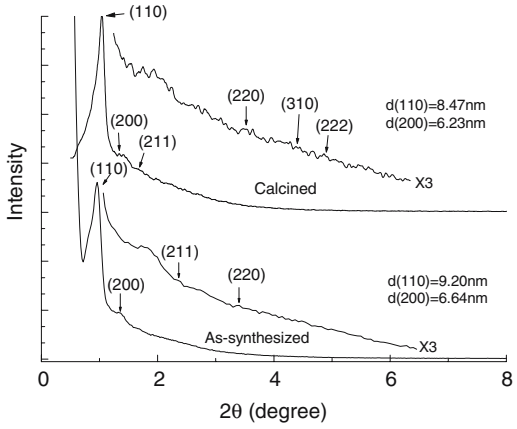

Fig. 3 X-ray diffraction patterns of the as-synthesized and the calcined mesoporous silicas prepared in a moderately acidic medium

TEM micrographs based on the (100) and the (110) planes of the calcined sample are presented in Fig. 4. One clearly observes well-ordered hexagonal arrays of pores for the sample prepared in this study. The channels of the sample are also noticed in other plane from the TEM images, which indicates a cage-type structure. These structures are characteristic of the SBA-16-type mesoporous silica.

Particle shape and size of the SBA-16-type mesoporous silica is a fairly important parameter for the application on the stationary phase for separation or catalysis. SEM micrographs of the calcined sample in Fig. 5 show that the prepared sample consists of uniform and highly perfect crystal particles with a diameter of 4–6 μm. All of these particles have morphologies of a rhombic dodecahedron, consisting of 12 well-defined crystal faces (see Fig. 5b). These 12 faces can be indexed as (110) planes, and the crystal particle exhibits a cubic $Im\ \bar{3}m$ point group symmetry. Combined with the XRD analysis and the comparison of the relative intensity of these observed peaks with that reported in the appropriate literature, we can conclude that the crystals prepared with the template of F108 type triblock copolymer in the moderately acidic media have $Im\ \bar{3}m$ symmetry.

The nitrogen adsorption–desorption isotherm and pore size distribution for the calcined sample are presented in Fig. 6, which belongs to Langmuir type IV according to the IUPAC classification. This type is characteristic of mesoporous materials with a narrow pore size distribution. The curve exhibits a very typical adsorption–desorption hysteresis with the desorption delay and the steepness of curve slope in the relative pressure (p/p_0) range of 0.40–0.45. This result is clearly indicative of characteristic cage-like pore structure, which has been examined in detail by P. I. Ravikovitch et al., and fully complies with the non local density functional theory [25]. The pore size

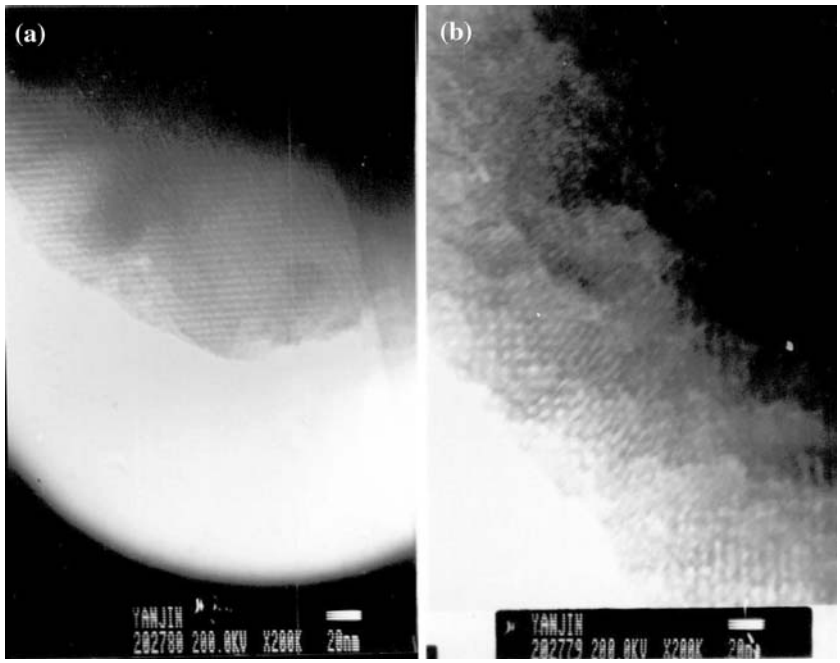

Fig. 4 TEM micrograph micrographs of the prepared mesoporous silica: (**a**) (100), and (**b**) (110) directions

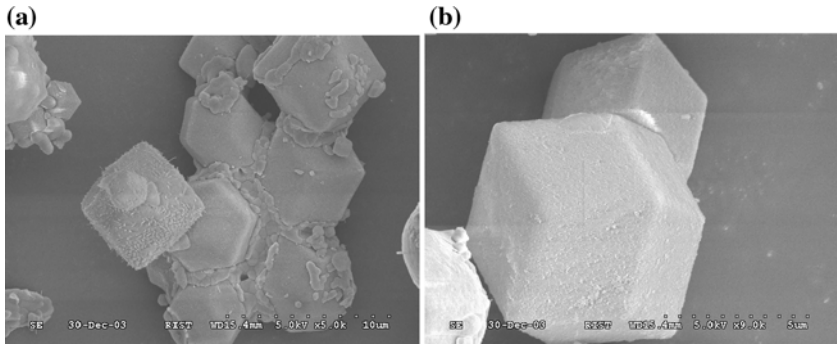

Fig. 5 SEM micrographs of the prepared mesoporous silica: (**a**) at low magnification, and (**b**) at high magnification

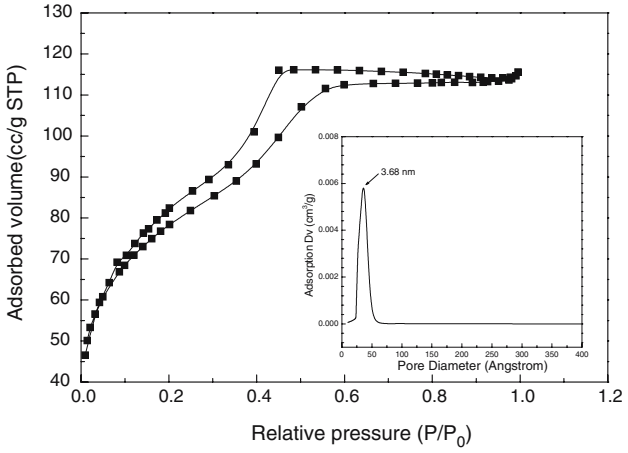

Fig. 6 Nitrogen adsorption–desorption isotherm and pore size distribution plots of the calcined mesoporous silica prepared in a moderately acidic medium

distribution, calculated from the adsorption isotherm, shows a narrow distribution of small mesopores, distributed around an average pore diameter of 3.68 nm. The total BET surface area is 363.648 m^2/g, and the total pore volume of this sample is 0.379 cm^3/g. The pore wall thickness (d_w) of the sample is calculated from the simple formula $d_w = \sqrt{3}a_0/2 - d_p$ where d_p and a_0 are the mesopore diameter and cubic unit cell parameter, respectively [26]. The wall thickness was calculated to be 6.63 nm. It is implied that such a thick pore wall provides a much better thermal stability for the mesoporous silica prepared in this study in comparison with the MCM type mesoporous materials.

In the present study, we successfully synthesized the SBA-16-type mesoporous silica with uniform small pores, thick pore walls, good cage-like connectivity, as well as highly perfect cubic crystal architecture. In contrast with the strongly acidic synthesis

conditions (2.0 mol/l HCl solution) for the SBA-16-type mesoporous silica reported by other numerous authors [9, 10, 23, 26], we prepared the SBA-16-type mesoporous silica materials by using the nonionic surfactant (EO_{132}–PO_{50}–EO_{132} triblock copolymer) as template in a moderately acidic media (0.5 mol/l HCl solution). It is well known that the silica source's hydrolysis reaction and the silicate's condensation reaction conditions determine the final porous and morphological architectures of the mesoporous silica. The pore size, wall thickness and microporosity of the mesoporous silica can usually be governed simply by silica concentrations in the reaction gel, whereas its morphology is difficult to be controlled [23]. A strongly acidic condition evidently accelerates the hydrolysis reaction as well as the condensation reaction, in which H^+ ions play a role as catalyst for both of them, but results in an irregular morphological construction. However, when the mesoporous silica was synthesized under moderately acidic conditions, the depression of the hydrolysis reaction and the condensation reaction seem to favor the formation of a highly regular crystal structure. On the other hand, the nonionic surfactants result in the formation of mesoporous silica through hydrogen bond or van der Waals interaction, in which the hydrogen-bonding interaction of nonionic triblock copolymer with the silica source is generated as a form of $(S^0H^+)(X^-I^0)$ under acidic conditions [27]. The moderately acidic media can reduce the assembly of silica source in the surface of micellar triblock copolymer, in comparison with the strongly acidic one, and subsequently increases the amount of silica source available for the framework of the mesoporous silica. As a result, a thick pore wall was achieved under this condition.

In summary, compared with the mesoporous silica materials prepared in strong acidic conditions, the SBA-16-type mesoporous silica crystals prepared under moderately acidic conditions have much smaller pores, thicker pore walls, and more highly regular crystal structures. Owing to its more characteristic structure than that of the mesoporous silica materials prepared by conventional methods, our preparations not only favor the industrial uses because of their case of synthesis, but they also may promote potential applications in catalysis, sensoring, and separation. Such applications are due to the prepared mesoporous silica's high microporosity within the inorganic framework. The large amount of silanols may favor the incorporation of catalytically active heteroatoms in silica frameworks, and the functionalization of organic groups.

Conclusion

Mesoporous silica crystals were successfully synthesized under moderately acidic conditions of 0.5 mol/l HCl solution. The essence of the SBA-16-type mesoporous materials with a 3D cage-like microporosity was evidenced by its well-defined XRD pattern combined with its TEM images. The SEM micrographs revealed highly regular cubic crystal architecture for the prepared mesoporous silica materials. The size of the crystal particles was maintained in the range 4–6 μm, which is a fairly important parameter for the application of the stationary phase for separation. The prepared mesoporous silica also possesses small pores with an average diameter of 3.68 nm, a total surface area of 363.648 m^2/g. The total pore volume is 0.379 cm^3/g, and the pore-wall thickness is 6.63 nm. These characteristics may lead to higher thermal and hydrothermal stability, excellent microporosity, and good connectivity. The mesoporous silica prepared in this study exhibits potential applications in catalysis, sensoring, and separation, as it can be propitious to be industrialized owing to its moderately synthesis condition.

Acknowledgements The authors greatly appreciate financial support from The National Nature Science Foundation of China (Grant No.: 50573006) and The Opening Fund of Key Laboratory of Beijing City on Preparation and Processing of Novel Polymer Materials.

References

1. Kresge CT, Leoniwics ME, Roth WJ, Vartuli JC, Beck JC (1992) Nature 359:710
2. Beck JS, Vartuli JC, Roth WJ, Leonowicz ME, Kresge CT, Schmitt KD, Chu CT-W, Olson DH, Sheppard EW, McCullen SB, Higgins JB, Schlenker JL (1992) J Am Chem Soc 114:10834
3. Liu P, Lee SH, Tracy TE, Yan Y, Turner JA (2002) Adv Mater 14:27
4. Yamada Y, Zhao H, Uchida H, Tomita M, Ueno Y, Ichino T, Honmu I, Asai K, Katsube T (2004) Adv Mater 14:812
5. Wirnsberger G, Yang P, Scott BJ, Chmelka BF, Stucky GD (2001) Spectrochim Acta A 57:2049
6. Zhao D, Yang P, Melosh N, Feng J, Chmelka BF, Stucky GD (1998) Adv Mater 10:1380
7. Schüth F, Schmidt W (2002) Adv Eng Mater 4:269
8. Zhao D, Yang P, Huo Q, Chmelka BF, Stucky GD (1998) Curr Opin Colloid Interface Sci 3:174
9. Zhao D, Feng J, Huo Q, Melosh N, Freddrickson GH, Chmelka BF, Stucky GD (1998) Science 279:548
10. Zhao D, Huo Q, Feng J, Chmelka BF, Stucky GD (1998) J Am Chem Soc 120:6024
11. Kruk M, Jaroniec M, Sayari A (1999) Micropor Mesopor Mater 27:217
12. Hunter HM, Wright PA (2001) Micropor Mesopor Mater 43:361
13. Sakamoto Y, Kaneda M, Terasaki O, Zhao D, Kim JM, Stucky GD, Shin HJ, Ryoo R (2000) Nature 408:449

14. Kim MJ, Ryoo R (1999) Chem Mater 11:487
15. Dai LX, Tabata K, Suzuki E (2001) Chem Mater 13:208
16. Stein A (2003) Adv Mater 15:763
17. Mercier L, Pinnavaia TJ (1997) Adv Mater 9:500
18. Kruk M, Antochshuk V, Matos JR, Mercuri LP, Jaroniec M (2002) J Am Chem Soc 124:768
19. Yu C, Tian B, Fan J, Stucky GD, Zhao D (2002) J Am Chem Soc 124:4556
20. Kruk M, Celer EB, Jaroniec M (2004) Chem Mater 16:698
21. Cheng CF, Lin YC, Cheng HH, Chen YC (2003) Chem Phys Lett 382:496
22. Dai LX, Tabata K, Suzuki E (2001) Chem Mater 13:208
23. Voort PVD, Benjelloun M, Vansant EF (2002) J Phys Chem B 106:9027
24. Messina P, Morini MA, Schulz PC (2004) Colloid Polym Sci 282:1063
25. Ravikoviticth PI, Neimark AV (2002) Langmuir 18:1550
26. Kruk M, Antochshuk V, Matos JR, Mercuri LP, Jaroniec M (2002) J Am Chem Soc 124:768
27. Wang L, Fan J, Tian B, Yang H, Yu C, Tu B, Zhao D (2004) Micropor Mesopor Mater 67:135